Experimental Section

Single crystals: Succinic acid (0.20 g; Aldrich) was dissolved in cyclohexanol (4.0 g; Acros) and carefully layered above water (5.0 g) containing $Ni(acetate)_2 \cdot 6H_2O$ (0.20 g; Alfa Aesar) inside a Teflon autoclave liner (23 mL). The autoclave was heated under autogenous pressure to 150 °C for 3 days and the product, pale blue-green hexagonal platelets, was separated by filtration. Powder samples for physical characterization were prepared in a similar manner by combining $Ni(acetate)_2 \cdot 6H_2O$ (Alfa Aesar), succinic acid (Aldrich), and water in a 1:2:50 molar ratio. In situ X-ray powder diffraction data were collected every 25 °C on a Phillips X-Pert powder diffractometer using $Cu_{K\alpha}$ radiation. Elemental analysis (%) calcd: C 24.5, H 2.6; found: C 23.7, H 2.4; the calculation assumes 0.6 surface water molecules per formula unit, as measured by TGA.

Crystal data for $[Ni_7(C_4H_4O_4)_6(OH)_2(H_2O)_2] \cdot 2H_2O$, rhombohedral, $R\bar{3}c$, $a = 21.040(1)$, $c = 45.860(4)$ Å, $V = 17581(2)$ Å^3, $Z = 18$, $\rho = 1.995$ Mg m^{-3}, $R_1 = 0.0444$ for 3290 reflections, $I > 4\sigma I$ for 267 least-squares parameters. Single-crystal diffraction data were collected to 0.75 Å on a clear, hexagonal crystal ($0.12 \times 0.12 \times 0.08$ mm) using a Bruker SMART CCD system with $Mo_{K\alpha}$ radiation (0.71073 Å). An absorption correction was made using SADABS.[20] Lorentz and polarization corrections were made, the structure was solved using direct methods, and the data were refined against $|F^2|$ using the SHELXTL suite.[21] All non-hydrogen atoms were refined anisotropically, and hydrogen atoms were placed in calculated positions with isotropic U values 20% higher than the atom to which they were bound. Crystallographic data (excluding structure factors) for the structure reported in this paper have been deposited with the Cambridge Crystallographic Data Centre as supplementary publication no. CCDC-169140. Copies of the data can be obtained free of charge on application to CCDC, 12 Union Road, Cambridge CB2 1EZ, UK (fax: (+44) 1223-336-033; e-mail: deposit@ccdc.cam.ac.uk).

Received: August 23, 2001 [Z17783]

[1] A. K. Cheetham, G. Férey, T. Loiseau, *Angew. Chem.* **1999**, *111*, 3466; *Angew. Chem. Int. Ed.* **1999**, *38*, 3269.
[2] T. J. Barton, L. M. Bull, W. G. Klemperer, D. A. Loy, B. McEnaney, M. Misono, P. A. Monson, G. Pez, G. W. Scherer, J. C. Vartuli, O. M. Yaghi, *Chem. Mater.* **1999**, *11*, 2633.
[3] R. Robson, *J. Chem. Soc. Dalton Trans.* **2000**, 3735.
[4] M. Eddaoudi, D. B. Moler, H. L. Li, B. L. Chen, T. M. Reineke, M. O'Keeffe, O. M. Yaghi, *Acc. Chem. Res.* **2001**, *34*, 319.
[5] H. Li, M. Eddaoudi, M. O'Keeffe, O. M. Yaghi, *Nature* **1999**, *402*, 276.
[6] S. S. Y. Chui, S. M. F. Lo, J. P. H. Charmant, A. G. Orpen, I. D. Williams, *Science* **1999**, *283*, 1148.
[7] L. M. Zheng, X. Q. Wang, Y. S. Wang, A. J. Jacobson, *J. Mater. Chem.* **2001**, *11*, 1100.
[8] J. Do, A. J. Jacobson, *Inorg. Chem.* **2001**, *40*, 2468.
[9] Y. Kim, E. W. Lee, D. P. Jung, *Chem. Mater.* **2001**, in press.
[10] Y. Kim, D. Y. Jung, *Bull. Korean Chem. Soc.* **2000**, *21*, 656.
[11] Y. J. Kim, D. Y. Jung, *Bull. Korean Chem. Soc.* **1999**, *20*, 827.
[12] C. Livage, C. Egger, G. Férey, *Chem. Mater.* **2001**, *13*, 410.
[13] C. Livage, C. Egger, G. Férey, *Chem. Mater.* **1999**, *11*, 1546.
[14] N. Guillou, Q. M. Gao, M. Nogues, R. E. Morris, M. Hervieu, G. Férey, A. K. Cheetham, *C. R. Acad. Sci. Ser. IIc* **1999**, *2*, 387.
[15] N. Guillou, Q. M. Gao, P. M. Forster, J. S. Chang, S. E. Park, G. Férey, A. K. Cheetham, *Angew. Chem.* **2001**, *113*, 2913; *Angew. Chem. Int. Ed.* **2001**, *40*, 2831.
[16] P. M. Forster, P. M. Thomas, A. K. Cheetham, *Chem. Mater.* **2002**, in press.
[17] K. Maeda, Y. Kiyozumi, F. Mizukami, *Angew. Chem.* **1994**, *106*, 2429; *Angew. Chem. Int. Ed. Engl.* **1994**, *33*, 2335.
[18] L. M. Zheng, T. Whitfield, X. Wang, A. J. Jacobson, *Angew. Chem.* **2000**, *112*, 4702; Angew. *Chem. Int. Ed.* **2000**, *39*, 4528.
[19] Unit cell: $I4_1/a$, $a = 24.0585$, $c = 16.6154$ Å.
[20] SADABS: Area-Detector Absorption Correction, Siemens Industrial Automation, Inc., Madison, WI, **1996**.
[21] SHELXTL v5.1, Bruker-AXS, Inc., Madison, WI, **1988**.

Icosahedral Virus Particles as Addressable Nanoscale Building Blocks**

Qian Wang, Tianwei Lin, Liang Tang, John E. Johnson,* and M. G. Finn*

Dedicated to Professor K. Barry Sharpless

Nanochemistry is the synthesis and study of well-defined structures with dimensions of 1 – 100 nanometers (nm), and thus spans the size range between molecules and materials.[1] While supramolecular chemistry (making small molecules bigger) and microfabrication techniques (making big structures smaller) attack from the flanks, biology employs many constructs of this size. Examples include the photosynthetic reaction center, the ribosome, and membrane-bound receptor-signaling complexes, all notable because of their sophisticated yet modular function. The burgeoning field of nanotechnology[2] seeks to mimic the information-handling, materials-building, and responsive sensing capabilities of biological systems at the nanometer scale. The special requirements of this enterprise would be well served by building blocks of the proper size with predictable and programmable chemistry.

Cowpea mosaic virus (CPMV) particles are 30 nm-diameter icosahedra, formed by 60 copies of two different types of protein subunits (Figure 1a).[3] The physical, biological, and genetic properties of CPMV have been well characterized.[4] Approximately one gram of virus is easily and routinely obtained from a kilogram of infected leaves of the black-eye pea plant. The structure of CPMV has been characterized at 2.8 Å resolution by X-ray crystallography and an atomic model of the particle has been constructed.[5] The virion displays icosahedral symmetry to the resolution of the crystal structure and an infectious clone of the virus allows site-directed and insertional mutagenesis to be performed in a straightforward and rapid manner.[6] The particles are remarkably stable; they maintain their integrity at 60 °C (pH 7) for at least one hour and at pH values from 3.5 to 9 indefinitely at room temperature. Different crystal forms of the virus can be readily produced under well-defined conditions (Figure 1d).[7, 8] Here we report on the selective

[*] Prof. M. G. Finn, Dr. Q. Wang
Department of Chemistry
The Scripps Research Institute
10550 N. Torrey Pines Rd., La Jolla, CA 92037 (USA)
Fax: (+1) 858-784-8850
E-mail: mgfinn@scripps.edu
Prof. J. E. Johnson, Prof. T. Lin, Dr. L. Tang
Department of Molecular Biology
The Scripps Research Institute
10550 N. Torrey Pines Rd., La Jolla, CA 92037 (USA)
Fax: (+1) 858-784-2980
E-mail: jackj@scripps.edu

[**] We thank The Skaggs Institute of Chemical Biology, the Naval Research Laboratory (N00014-00-1-0671), and the National Institutes of Health (GM344220-18 and A147823-01) for support of this work. Q.W. is a Skaggs Postdoctoral Fellow. We are also grateful to Dr. Gino Cingolani for data collection at the Stanford Synchrotron Radiation Laboratory (SSRL is operated by the U.S. Department of Energy, Office of Basic Energy Sciences), and Prof. R. Lerner and Dr. D. Kubitz for a gift of antibody 19G2.

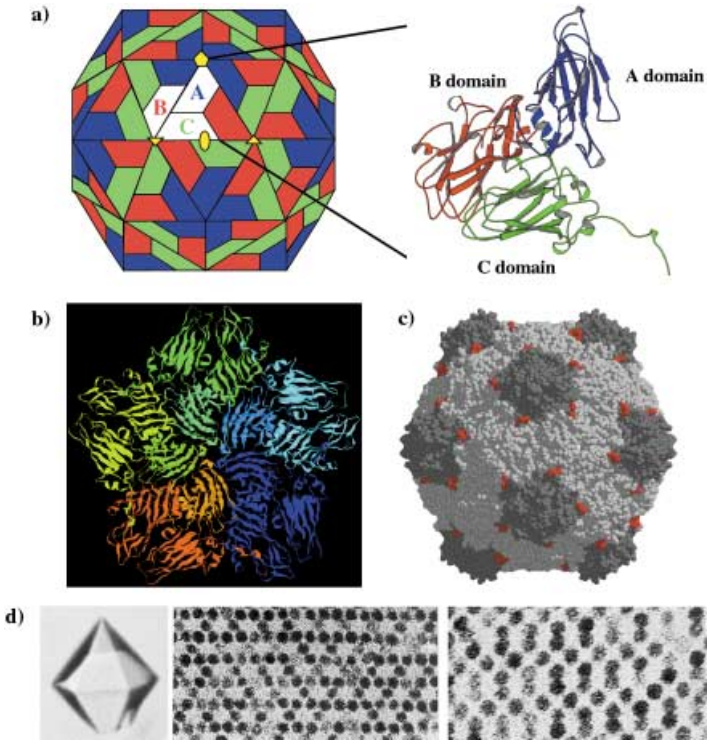

Figure 1. Structure of cowpea mosaic virus and its crystals. a) Left: A diagramatic representation of CPMV which shows the distribution of the two subunits that comprise the "asymmetric unit", 60 copies of which form the icosahedral particle. The trapezoids in red and green represent the two domains of the large subunit clustered around the threefold symmetry axes and the blue trapezoid represents the small subunit clustered about the fivefold symmetry axes. Right: The folds of the two subunits. b) Organization of five asymmetric units into the "pentamer" centered around a small hole at each fivefold axis. c) Representation of the X-ray crystal structure of CPMV that highlights the EF-loop (in red) in the large subunit in which the cysteine-containing insert is made. d) Left: A hexagonal crystal of CPMV. Electron micrographs of crystals thin sectioned perpendicular to the *c* axis (middle) and the *a* axis (right) showing the remarkably open lattice. Previous studies have shown that proteins with dimensions in excess of 50 Å can be reversibly soaked into the crystals. A typical crystal contains 10^{13} particles.

chemical derivatization of the native virus and the crystal structure of a derivatized particle as well as the preparation of site-specific mutations that allow the attachment of fluorescent dyes and gold clusters through maleimide linkers. The results of these studies demonstrate that the virus particles can be exploited as addressable nanoblocks imbued with a variety of chemical and physical properties.[9]

Thiol-selective chemical reagents were used to probe the reactivity of non-disulfide-linked cysteine residues in the native virus particle. The crystal structure shows that CPMV has no free sulfhydryl groups on the outer surface[5] and there was no evidence of reaction with the commercially available monomaleimido-Nanogold reagent (Nanoprobes, Inc., Yaphank, NY) that has a molecular diameter of 1.4 nm. However, adducts of the native virus with ethyl mercury phosphate (EMP), an agent with a strong affinity for free sulfhydryl groups but with a dimension of only a fraction of a nanometer, were readily formed. The resulting labeled virus was crystallized under conditions previously employed.[7] Crystals with rhombic dodecahedral morphology, identical to those obtained with native virus, were obtained in four days and X-ray diffraction data to 6 Å resolution were collected on beam line 11–1 at the Stanford Synchrotron Radiation Laboratory. Figure 2a shows a pentamer of the icosahedral constellation of EMP molecules visualized in a difference electron density map. Figure 2b, c shows that the EMP reacted with a single CYS residue at position 295, on the *interior* surface of the large subunit. This residue contains the sulfhydryl group that appears in the X-ray crystal structure of CPMV to be the most exposed to solvent.[10]

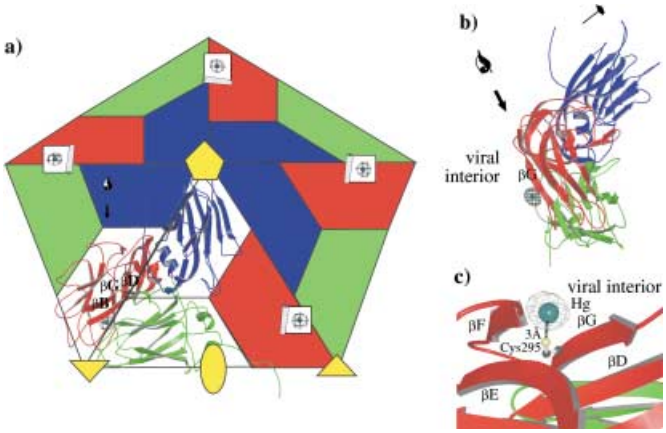

Figure 2. Crystallographic analysis of CPMV particles derivatized with EMP. Amplitudes in the Fourier series calculation were obtained by subtracting structure amplitudes computed from the atomic model of native CPMV from the measured structure amplitudes of the EMP derivative. The difference amplitudes and native phases were used to compute electron density. a) The pentameric assembly of CPMV protein about the fivefold symmetry axis. The difference electron density map reveals bound EMP molecules to be located solely at a single position below the outer capsid surface that corresponds to CYS295; five such sites are shown here. b) A view of the fold of the CPMV asymmetric unit with EMP difference density. c) A close-up view of the position of the EMP difference density.

The reactivity of native CPMV toward an organic thiol-selective reagent was found to be different than toward mercuric ion. Thus, wild-type CPMV was condensed with 5-maleimidofluorescein (**1**). Figure 3 shows a plot of the number of molecules of dye attached to native CPMV as a function of increasing concentration of the dye reagent.[11] The curve plateaus at 60 attached dye molecules per particle, which suggests that a single cysteine residue per icosahedral asymmetric unit is most reactive. Denaturing gel electrophoresis analysis of the derivatized protein (Figure 3) showed that the dye is attached exclusively to the *small* subunit, not to the large subunit as was the case for reaction of EMP at CYS295. This alkylation reaction must also occur on the interior capsid surface (see below), but its exact position has not yet been established. Multiple interior cysteine sites, on both small and large subunits, can be addressed with **1** at higher dye-to-subunit ratios without damaging the structural integrity of the particle (data not shown). Small molecules such as **1** are thus apparently able to diffuse through the

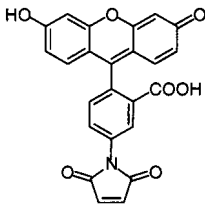

1

  1433-7851/02/4103-0460 $ 17.50+.50/0

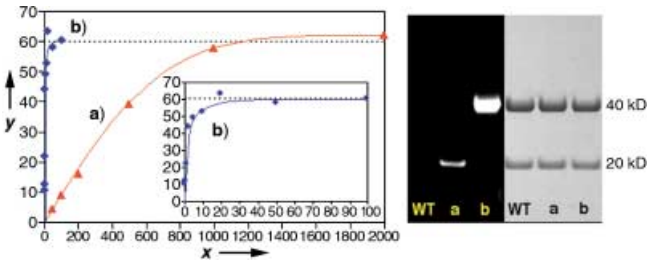

Figure 3. Left: Plots showing the number of the covalently attached fluorescein molecules to (a) native CPMV and (b) the CYS insertional mutant virus as a function of increasing ratio of reagent **1** to virus (x = equivalents dye–maleimide used per asymmetric unit; y = dyes attached per particle). Stoichiometries were determined by absorption measurements on solutions of labeled particles by comparison of the intensities of the dye (494 nm) to protein (260 nm), each of which have non-overlapping bands with well-established molar absortivities. Right: SDS-PAGE analysis: (WT) wild-type CPMV; a) wild-type CPMV-**1** conjugate having approximately 17 dye molecules attached per capsid; b) mutant CPMV-**1** conjugate containing 60 dyes per capsid. On the left (black background) is the gel visualized directly under UV light; this shows the fluorescein emission localized in the small protein subunit of the wild-type virus and the large subunit of the mutant. On the right (light background) is the gel visualized after Coumassie blue staining; this shows both small and large subunits.

capsid, perhaps through the small hole that appears in the crystal structure at each fivefold symmetry axis (Figure 1b).

Mutant CPMV particles were prepared to display sulfhydryl groups on the exterior surface of the structure. Thus, a five-residue insertion containing cysteine (GGCGG) was placed between positions 98 and 99 in the large subunit (Figure 1c). Yields comparable to wild type were obtained with this virus, but the presence of β-mercaptoethanol or tris(2-carboxyethyl)phosphane was required throughout the isolation procedure to avoid crosslinking of particles when they were pelleted by ultracentrifugation or stored after purification. These particles were treated with increasing concentrations of fluorescent dye; the results are shown in Figure 3. In the presence of smaller quantities of the dye-maleimide reagent, up to 60 dye molecules were attached per CPMV virion at significantly faster rates than were observed with the native particle. The reactive interior CYS residue remains active in the mutant particle, such that the two positions can be addressed sequentially under controlled conditions. Thus, reaction with 50 equivalents of **1**, followed by purification and reaction with 1000 equivalents of 5-maleimide tetramethylrhodamine (**2**), gave CPMV decorated with an average of 55 fluoresceins and 49 rhodamines per particle, as determined by UV/Vis spectroscopy.[11]

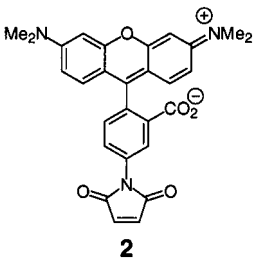

2

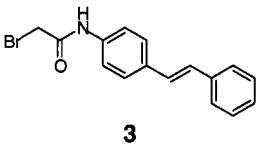

3

The differential properties of the reactive cysteine residues of wild-type vs. the mutant virus were probed by using the stilbene derivative **3** and antibodies to the stilbene moiety recently developed (Figure 4).[12] Since the bromoacetamide group of **3** is selectively reactive with cysteine sulfhydryl groups under conditions similar to those used for maleimides, CPMV-stilbene conjugates were readily prepared and purified for native and mutant virus particles. When treated with antibody 19G2, the presence of an antibody–stilbene complex is revealed by blue fluorescence upon excitation with a hand-held UV lamp; no fluorescence is observed in the absence of either stilbene or antibody. Figure 4 shows the results for intact and denatured CPMV conjugates of **3**. The successful attachment of the stilbene group to both wild-type and mutant CPMV was shown by the appearance of strong fluorescence when the denatured samples were treated with the antibody. The mutant CPMV–**3** conjugate similarly showed antibody binding to stilbene on the intact particle, but the wild-type CPMV–**3** conjugate did not. This is consistent with the attachment of **3** to the interior capsid surface of the wild-type virus, where it is inaccessible to the indicating antibody. In contrast, the mutant virus displays its stilbene-decorated cysteine residues to solvent on the exterior surface.

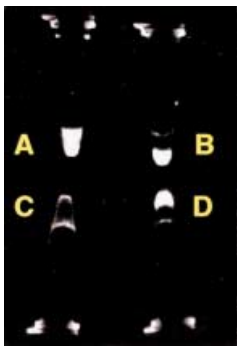

Figure 4. Black-and-white photograph of samples under UV irradiation: A) mutant CPMV-**3** conjugate + stilbene-binding antibody 19G2; B) denatured mutant CPMV-**3** conjugate + 19G2; C) wild-type CPMV-**3** conjugate + 19G2; D) denatured wild-type CPMV-**3** conjugate + 19G2. Note that denaturation causes precipitation of the viral protein, but exposed stilbenes are still recognized by the antibody.

The mutant virus was also treated with monomaleimido-Nanogold, providing virions displaying absorbance at 420 nm, which indicates attachment of the gold cluster. Derivatized particles were flash frozen and examined by electron microscopy and a three-dimensional image reconstruction was computed (Figure 5a).[13] Figure 5b shows a difference map in which density for the model CPMV structure was subtracted from the density computed in the image reconstruction. The gold particles are clearly visible at the positions of the inserted cysteine residues (Figure 5c), providing an example of the installation of chemical structures at designated positions on the icosahedral protein template.

We have shown here for the first time that a virus can function as a convenient and programmable platform for organic chemical reactions. Derivatized CPMV particles will generally display 60 copies of the attached molecule, which makes these systems analogous to very large dendrimers.[14] High local concentrations of the attached chemical agent are thereby engineered in the vicinity of the particle, which may result in novel chemical and/or biological properties. Appropriate choices of derivatizing agents can selectively target residues on the inner or outer surface of the particle, which allows double labeling of the particles with different molecules. We are continuing to expand the range of reactivity of CPMV with different mutational insertions and chemical derivatizing agents, with the goal of engineering novel function within a single particle and for aggregates of particles. For example, the virus surface can be patterned with metal nanoparticles if multiple cysteine residues are placed at accessible positions. Such a pattern could potentially

  1433-7851/02/4103-0461 $ 17.50+.50/0

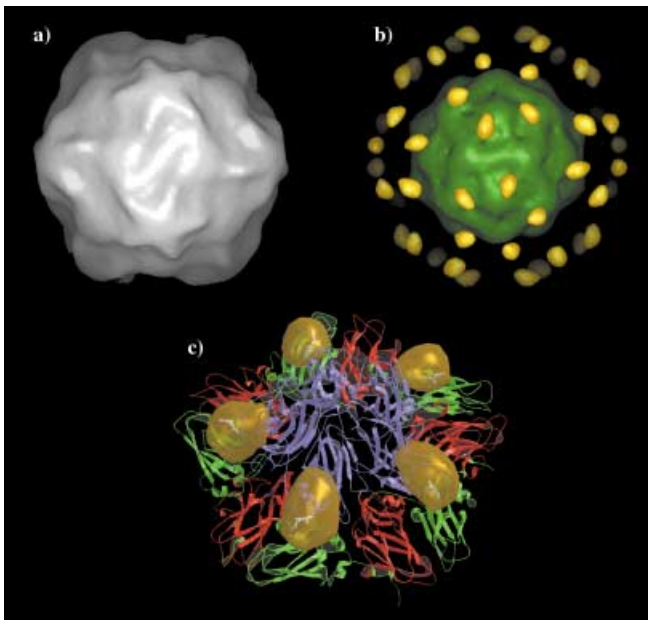

Figure 5. Cryo electron microscopy analysis of derivatized CPMV CYS mutant. a) Three-dimensional reconstruction of CPMV particles at 29 Å resolution labeled with 1.4 nm nanogold clusters. b) Difference electron density map generated by subtracting density computed with the native CPMV X-ray structure from the density shown in Figure 5a. Since the computed native CPMV density was made from only protein, the nucleic acid (shown in green) is visible in the difference map as well as the gold particles. c) A pentameric section of the difference electron density map around the fivefold symmetry axis superimposed on the atomic model of CPMV showing that the gold is attached at the site of the CYS mutation.

be used to form a conducting "wire" at the nanometer scale. Furthermore, CPMV icosahedra show a propensity for self-organization. Straightforward crystallization procedures lead to well-ordered arrays of 10^{13} particles in a typical 1 mm^3 crystal, which may be regarded as a meso scale self-organization of nanoblock components.[15] Thus, we believe that CPMV and other viruses have a rich future in applications spanning the worlds of molecular, biological, and materials science.

Experimental Section

Typical procedure for chemical derivatization of CPMV (unless otherwise noted, "buffer" refers to 0.1M potassium phosphate, pH 7.0): Virus (1 mg mL^{-1} in buffer) and maleimide reagent at the indicated concentration were incubated in an 80:20 buffer/DMSO mixture at 4 °C for 6 to 48 h; all reactions contributing to Figure 3 were run for a constant time of 24 h. Reaction mixtures were purified on small scale (80 μL) by passage through short-size exclusion columns prepared with Bio-Gel P-100 Gel (Bio-Rad) in buffer, packed in Bio-Spin disposable chromatography columns, and eluted at 1000 g for 3 minutes. Multiple passages through freshly-packed columns were performed until dye was undetectable in the wash solution and the relevant absorbance ratios for the virus samples were constant. Purification of larger quantities of derivatized virus was performed by repeated ultracentrifugation pelleting and resuspension in buffer. Yields of labeled virus particles after purification were 70–80%. For quantitation, the "effective" absorptivity (ε) of the dye was independently measured by constructing a calibration curve with varying amounts of dye in a buffer solution containing the same concentration of wild-type CPMV as used in the attachment reactions. The experimental error in the number of attached dye molecules is ±10% of the reported value. The intact nature of the derived particles was substantiated by sucrose gradient ultracentrifugation and size-exclusion FPLC chromatography (Superose-6); nonspecific dye adsorption to the virus was ruled out by appropriate control experiments.

Nanogold labeling: Monomaleimido-Nanogold (Nanoprobes, Inc., 6 nmol) was dissolved in 2-propanol (10 μL). The resulting dark brown solution was mixed with the cysteine mutant virus (60 μg) in 0.1M potassium phosphate buffer (pH 6.0, 90 μL, containing 10 mM tris(2-carboxyethyl)phosphane). After 20 h at 4 °C, the reaction mixture was purified by passage through size-exclusion gel as described above. The product was collected as a colorless solution (100 μL) with virus concentration = 0.45 mg mL^{-1}, which was used directly for the cryo electron microscopy study.

Received: September 13, 2001 [Z17898]

[1] G. M. Whitesides, J. P. Mathias, C. T. Seto, *Science* **1991**, *254*, 1312–1319; colloidal particles of 1–100 nm dimension are usually not considered to be nanochemical components because of their amorphous nature.
[2] For reviews of nanotechnology, see: a) the September, **2001**, issue of *Scientific American*; b) K. E. Drexler, "Nanosystems: Molecular Machinery, Manufacturing, and Computation", Wiley-Interscience, New York, **1992**; c) C. M. Niemeyer, *Angew. Chem.* **2001**, *113*, 4254–4287; *Angew. Chem. Int. Ed.* **2001**, *40*, 4128–4158.
[3] J. E. Johnson, J. Speir, *J. Mol. Biol.* **1997**, *269*, 665–675.
[4] G. Lomonossoff, M. Shanks, C. Holness, A. Maule, D. Evans, Z. Chen, C. Stauffacher, J. E. Johnson in *Biochemistry and Molecular Biology of Plant–Pathogen Interactions* (Ed.: C. J. Smith), Clarendon, Oxford, **1991**, pp. 76–91.
[5] T. Lin, Z. Chen, R. Usha, C. V. Stauffacher, J.-B. Dai, T. Schmidt, J. E. Johnson, *Virology* **1999**, *265*, 20–34.
[6] G. P. Lomonossoff, J. E. Johnson, *Curr. Opin. Struct. Biol.* **1996**, *6*, 176–182; T. Lin, C. Porta, G. Lomonossoff, J. E. Johnson, *Fold. Des.* **1996**, *1*, 179–187.
[7] J. White, J. E. Johnson, *Virology* **1980**, *101*, 319–324.
[8] J. E. Johnson, C. Hollingshead, *J. Ultrastruct. Res.* **1981**, *74*, 223–231.
[9] The exciting potential of plant viruses as components of hybrid inorganic materials is being explored by Douglas, Young, and coworkers. See: T. Douglas, M. Young, *Adv. Mater.* **1999**, *11*, 679–681; and W. Shenton, T. Douglas, M. Young, G. Stubbs, S. Mann, *Adv. Mater.* **1999**, *11*, 253–256.
[10] Preliminary studies of proteolytic digestion of CPMV show it to possess a relatively rigid capsid (in contrast, see: B. Bother, X. F. Dong, L. Bibbs, J. E. Johnson, G. Siuzdak, *J. Biol Chem.* **1998**, *273*, 673–676; B. Bothner, A. Schneemann, D. Marshall, V. Reddy, J. E. Johnson, G. Siuzdak, *Nat. Struct. Biol.* **1999**, *6*, 114–116). While we do not discount potential capsid dynamics, we believe the X-ray data provide a reliable guide to the structure of the particle in solution.
[11] A solution of 1 mg mL^{-1} CPMV (average molecular weight 5.6×10^6 including encapsidated RNA) is 0.18 μM in virus *particles* and (0.18 × 60) = 11 μM in viral protein, defined as the concentration of the asymmetric unit (molecular weight 66000). In Figure 3 and the text, the amount of dye–maleimide (**1**) used is given in terms of its molar ratio to the amount of viral protein, whereas the number of dye molecules attached is reported in terms of dyes per virus particle.
[12] A. Simeonov, M. Matsushita, E. A. Juban, E. H. Z. Thompson, T. Z. Hoffman, A. E. I. Beuscher, M. J. Taylor, P. Wirsching, W. Rettig, J. K. McCusker, R. C. Stevens, D. P. Millar, P. G. Schultz, R. A. Lerner, K. D. Janda, *Science* **2000**, *290*, 307–313.
[13] For other uses of Nanogold in electron microscopy imaging, see: J. F. Hainfeld, R. D. Powell, *Cell Vision* **1997**, *4*, 408–432; R. A. Milligan, M. Whittaker, D. Safer, *Nature* **1990**, *348*, 217–221; J. Crum, K. J. Gruys, T. G. Frey, *Biochemistry* **1994**, *33*, 13719–13726; J. F. Hainfeld, *Science* **1987**, *236*, 450–453.
[14] We also wish to call attention to the engineered protein assemblies of Yates and coworkers (J. E. Padilla, C. Colovos, T. O. Yeates, *Proc. Natl.Acad. Sci. USA* **2001**, *98*, 2217–2221). This work illustrates the potential for the nonbiological design of viruslike particles, which should also be viable templates for chemical manipulation.
[15] In terms of their overall appearance and properties of aggregation, the plastic polyhedra of Whitesides bear a striking resemblance to icosahedral plant viruses. See: N. B. Bowden, M. Weck, I. S. Choi, G. M. Whitesides, *Acc. Chem. Res.* **2001**, *34*, 231–238; T. L. Breen, J. Tien, S. R. Oliver, T. Hadzic, G. M. Whitesides, *Science* **1999**, *284*, 948–951.

  1433-7851/02/4103-0462 $ 17.50+.50/0